

## EFFECT OF SUBSTRATE TEMPERATURE ON STRUCTURAL AND OPTICAL PROPERTIES OF ZINC ALUMINUM OXIDE THIN FILMS PREPARED BY DC REACTIVE MAGNETRON SPUTTERING TECHNIQUE

B. RAJESH KUMAR<sup>a,b\*</sup>, T. SUBBA RAO<sup>b</sup>

<sup>a</sup>*Department of Physics, Sri Venkateswara University, Tirupati-517502, A.P, India*

<sup>b</sup>*Materials Research Lab, Department of Physics, Sri Krishnadevaraya University, Anantapur-515055, A.P, India*

Zinc Aluminum Oxide (ZAO) thin films were prepared by DC reactive magnetron sputtering on glass substrates and the effect of substrate temperature (from 303K-623K) on the structural and optical properties were studied. XRD patterns of ZAO thin films deposited at different substrate temperatures exhibit (0 0 2) preferential orientation with the c-axis perpendicular to the substrate. SEM images of Zinc Aluminum Oxide thin films shows the grains are spherical in shape with an average grain size of ~0.4-1 $\mu$ m. Optical parameters such as absorption coefficient ( $\alpha$ ), extinction coefficient (k) and optical band gap ( $E_g$ ) were determined from the transmission data. The absorption coefficient values are in order of  $10^6\text{cm}^{-1}$ . The extinction coefficient value of the films varies from 0.02 to 0.08. The direct optical band gap ( $E_g$ ) value of ZAO thin films are found to be in the range of 3.17-3.43eV.

(Received October 31, 2011; accepted November 25, 2011)

*Keywords:* ZAO thin films, DC magnetron sputtering, Scanning electron microscope, Transmittance, Optical parameters

### 1. Introduction

Zinc oxide and doped zinc oxide films have extensive attention in recent years due to their excellent optical and electrical properties [1-3]. Group III metal-doped ZnO materials, particularly the Al-doped ZnO have attracted the intense interest for its great potential applications in the optically transparent conducting layers as the electrode for thin-film solar cells [4-7]. When ZnO films are doped with the appropriate metal atoms such as Al, Sn, Cd, Ga, In, etc., their conductivity can be changed from values as low as  $10^{-10} (\Omega \text{ cm})^{-1}$  to values as high as  $10^4 (\Omega \text{ cm})^{-1}$ . The wide range of conductivities and conductivity changes upon different environmental conditions make ZnO films suitable materials for oxidant gas sensing layers [8-10]. Zinc Aluminum Oxide (ZAO) films have been studied as a window layer for silicon thin films solar cells owing to its easily textured surface for efficient light trapping [11-13]. ZAO films are also wide band gap semiconductors ( $E_g=3.4-3.9\text{eV}$ ), which show optical transmission in the visible and near-infrared (IR) regions [14-17].

ZAO thin films can be produced by various deposition techniques, including pulsed laser deposition [18], chemical vapor deposition [19], sol-gel process [20], spray pyrolysis [21], evaporation [22], and magnetron sputtering [23]. Among the methods, magnetron sputtering has several advantages, such as low processing temperature, good adhesion of films on substrates, very good thickness uniformly, high deposition rate and high density of the films with relative ease of scaling to large areas. It is also a simple process, and the process parameters are easy to control. In

---

\*Corresponding author: rajphyind@gmail.com

the present work, we report a study of structural and optical properties of ZAO thin films deposited on glass substrates by dc magnetron sputtering from 303K to 623K.

## 2. Experimental details

Zinc Aluminum oxide thin films were prepared by DC reactive magnetron sputtering technique. High purity metal targets of Zinc (99.999%) and Al (99.99%) with 2 inch diameter and 4mm thickness are used for deposition on glass substrates. The base pressure in chamber was  $5 \times 10^{-4}$  Pa and the distance between target and substrate was set at 60 mm. The glass substrates were ultrasonically cleaned in acetone and ethanol, rinsed in an ultrasonic bath in deionized water for 15 min, with subsequent drying in an oven before deposition. High purity (99.999%) Ar and O<sub>2</sub> gas was introduced into the chamber and was metered by mass flow controllers for a total flow rate fixed at 30 sccm. Deposition was carried out at a working pressure of 1 Pa after pre-sputtering with argon for 10 min. For the Zinc Aluminum Oxide thin films deposition, O<sub>2</sub> flow rate is 2 sccm and the deposition time is 30 min. The sputtering power was maintained at 110 W during deposition. The depositions were carried out with substrate temperatures from 303 K to 623 K. Film thickness was measured by Talysurf thickness profilometer. The resulting thickness of all the films is about 400 nm. The optical transmittance measurements were carried out using Cary 5E UV-VIS-NIR spectrophotometer. Surface morphology of the samples has been studied using Hitachi SU6600 Variable Pressure Field Emission Scanning Electron Microscope (FESEM) with Energy Dispersive Spectroscopy (Horiba, EMAX, 137 eV). EDS is carried out for the elemental analysis of prepared thin film samples.

## 3. Results and discussion

Fig. 1 shows X-ray diffraction (XRD) plots of ZAO films deposited on glass substrates from 303 K–623 K, it exhibits peaks at  $\sim 34.36^\circ$ – $34.6^\circ$  correspond to (0 0 2) phases. The (0 0 2) preferred orientation is due to the minimal surface which the hexagonal structure, c-plane of ZnO crystallites, corresponds to the densest packed plane [24]. In the present case of ZAO films deposited on glass substrates, the internal stresses were predominantly compressive. The internal compressive stresses in the films deposited by using sputtering method are thought due to the “atomistic peening” effect by the bombardment of energetic species during deposition [25]. It can be seen that the peak intensities are very weak and almost same. Because the glass substrate is amorphous, the ZAO films deposited on glass also show poor crystallinity. Therefore, the atomistic peening phenomenon is considered to occur weakly, so the stress difference due to the pressure variation is very small.

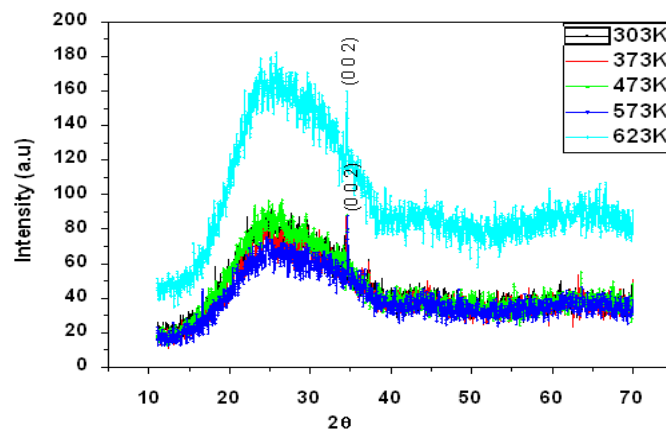


Fig 1. XRD patterns of ZAO thin films deposited on glass substrates at different substrate temperatures.

Fig. 2(a)-(e) shows Scanning electron microscopy (SEM) images of ZAO thin films deposited on glass substrate at different substrate temperatures. SEM images have clear spherical grains with an average grain size of  $\sim 0.4\text{-}1\mu\text{m}$ . Energy Dispersive Spectrum (EDS) with compositional elemental data is shown in figure 3(a)-(e). From EDS data the atomic percentage of Aluminum(Al) is more than 10% which causes the crystallinity of the films to deteriorate, which may be due to the formation of the stresses by the difference in ion size between zinc and the dopant of impurity atoms(Al) [26,27].

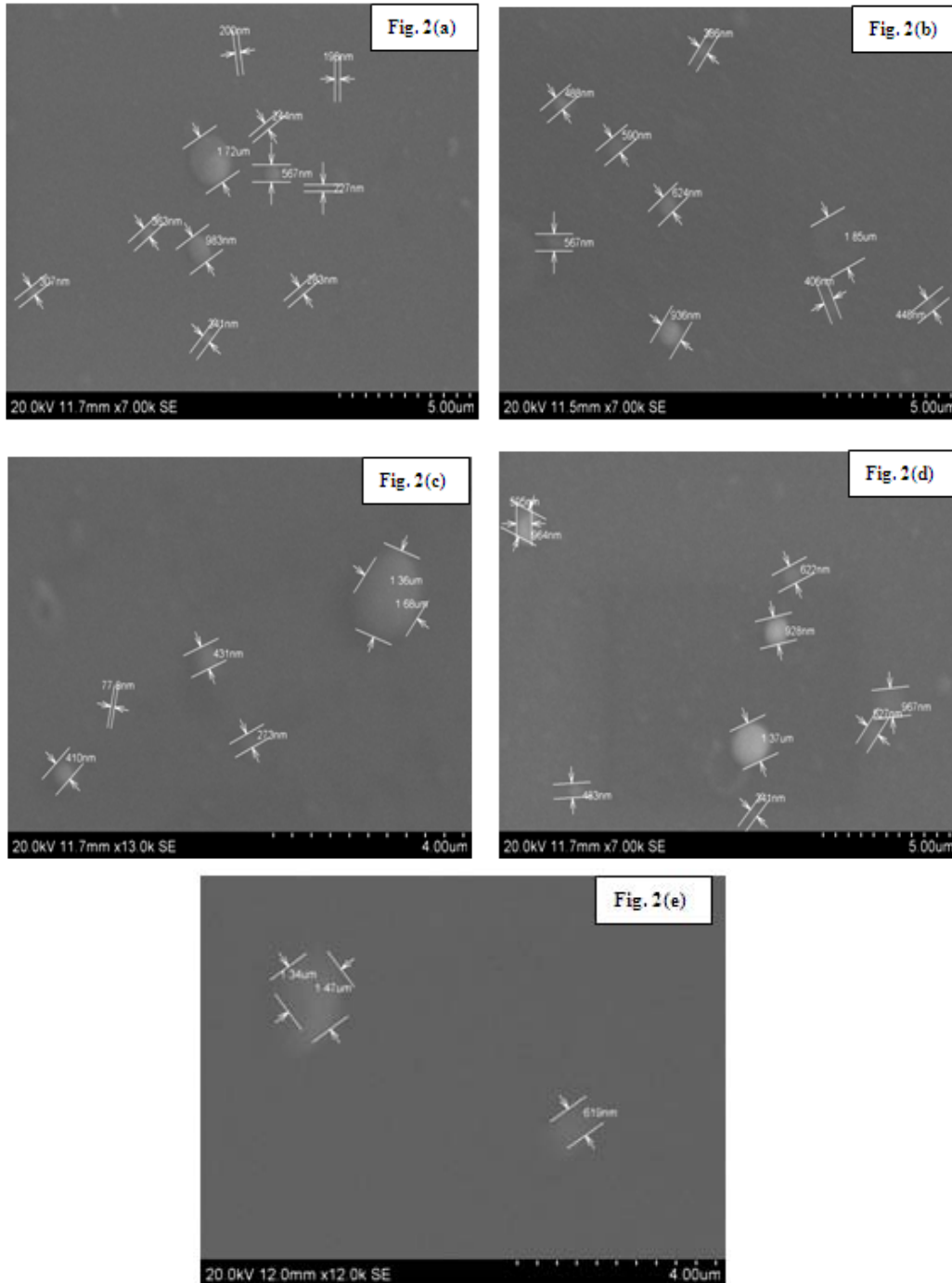


Fig 2. Scanning Electron Microscopy (SEM) image of ZAO thin films deposited on glass substrates at temperatures (a) 303K (b) 373K (c) 473K (d) 573K and (e)623K

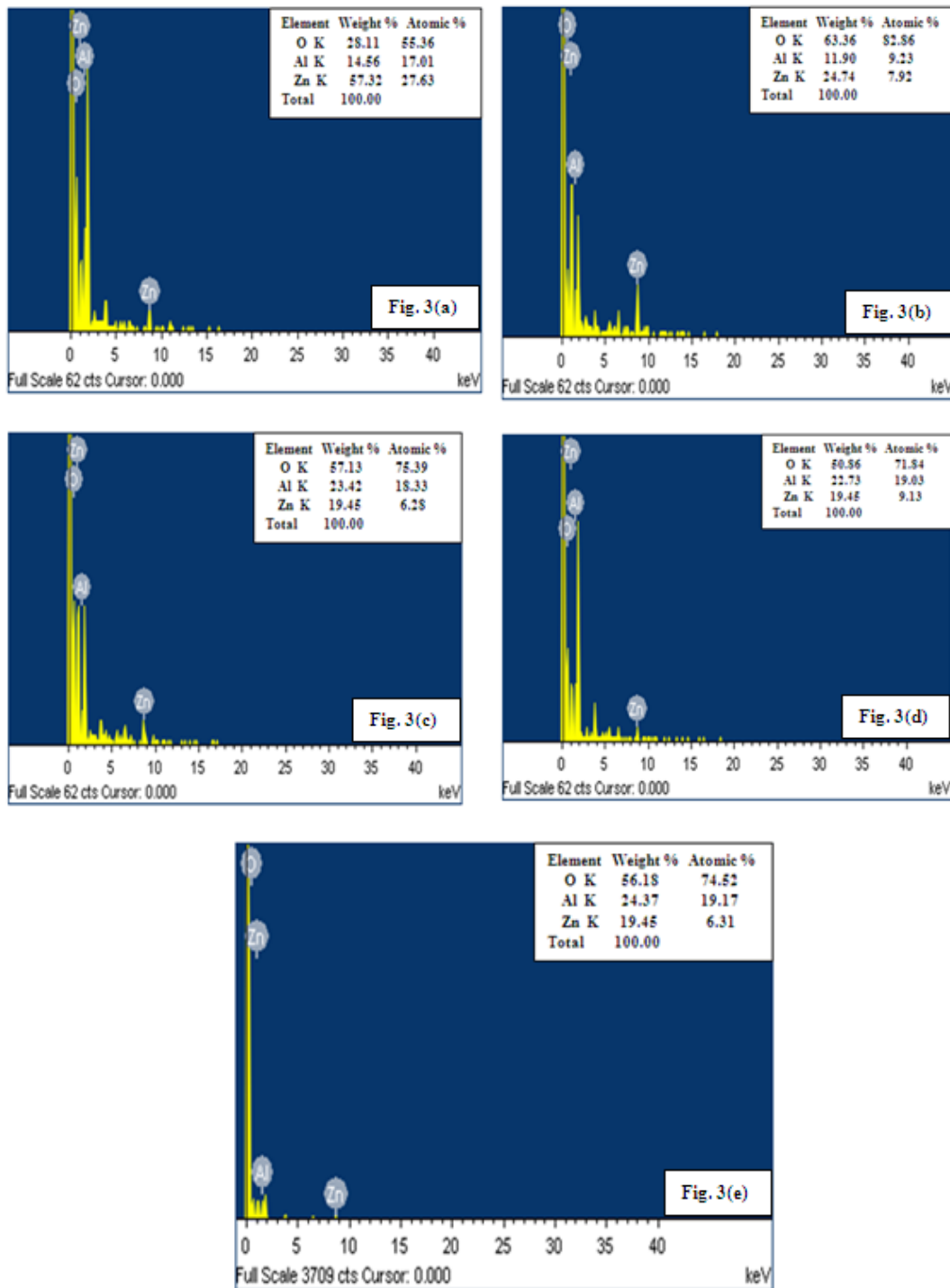


Fig 3. EDS plots of ZAO thin films deposited on glass substrates at temperatures (a) 303K (b) 373K (c) 473K (d) 573K and (e) 623K

The optical transmittance spectra of Zinc Aluminum Oxide (ZAO) films deposited on glass substrates from room temperature (303K) to 623K is shown in figure 4. ZAO film deposited at room temperature has a relatively low transmittance. The film deposited at 373K had a transmittance of nearly 85% in visible spectra region. The optical transmittance is decreased with increase of substrate temperature from 303K to 623K. For the films prepared at higher substrate

temperatures, transmittance shows a consistent decrement at higher wavelengths due to more aluminum content.

The absorption edge of the transmittance shifted to the shorter wavelength region upto the substrate temperature of 373K. This result is believed to be due to the Burstein-Moss effect hypothesis, which predicts that the fermi level inside the conduction band moves upward with increasing donor concentration due to the filling of the conduction band by the increase of electron carriers. It is known that the optical band gap is proportional to the carrier concentration.

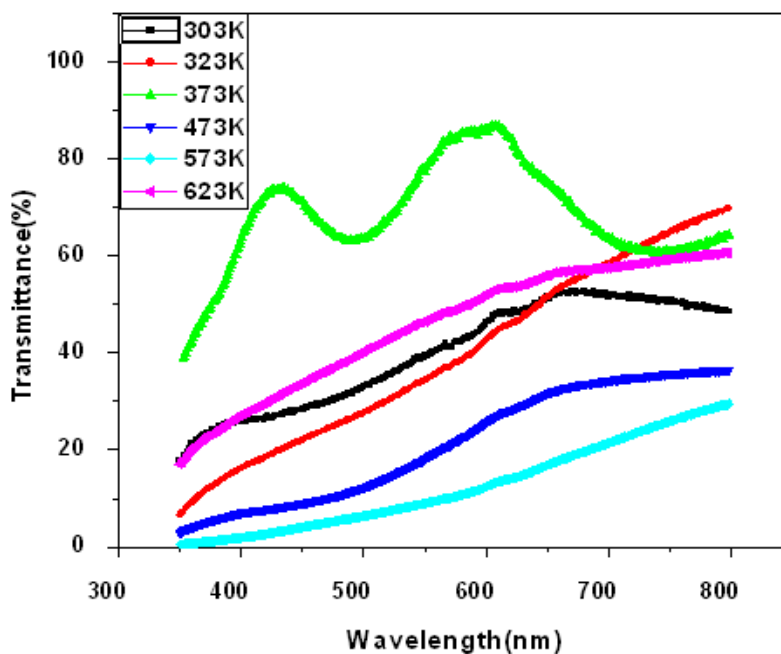


Fig. 4. Optical transmittance spectra of ZAO films at different substrate temperatures

Optical parameters such as absorption coefficient ( $\alpha$ ), extinction coefficient ( $k$ ) and optical band gap ( $E_g$ ) were determined from the transmission data. The extinction coefficient ( $k$ ) can be calculated by using the relation [28].

$$k = \frac{\alpha d}{4\pi} \quad (1)$$

where  $\alpha$  is the absorption coefficient and is calculated from the relation

$$\alpha = \frac{1}{d} \ln \left( \frac{1}{T} \right) \quad (2)$$

where  $d$  is the thickness of the film and  $T$  is the transmittance [29].

Figure 5 shows the variation of the absorption coefficient ( $\alpha$ ) as a function of wavelength ( $\lambda$ ) for the films deposited on glass substrate at different substrate temperatures. Absorption coefficient ( $\alpha$ ) decreases with increase of wavelength ( $\lambda$ ). The maximum absorption coefficient is obtained for the thin film deposited at 473K. The absorption coefficient ( $\alpha$ ) is found to be in order of  $10^6 \text{ cm}^{-1}$  at shorter wavelength regions. For higher values of photon energy, the energy dependence of absorption coefficient ( $\alpha > 10^4 \text{ cm}^{-1}$ ) suggests the occurrence of direct electron transitions. The extinction coefficient increases with the increase in energy of the incident beam. The values of extinction coefficient ( $k$ ) with wavelength ( $\lambda$ ) are found to be in the range of 0.02-

0.08. Optical absorption edge of Zinc Aluminum oxide films has a significant blue shift to the region of higher photon energy.

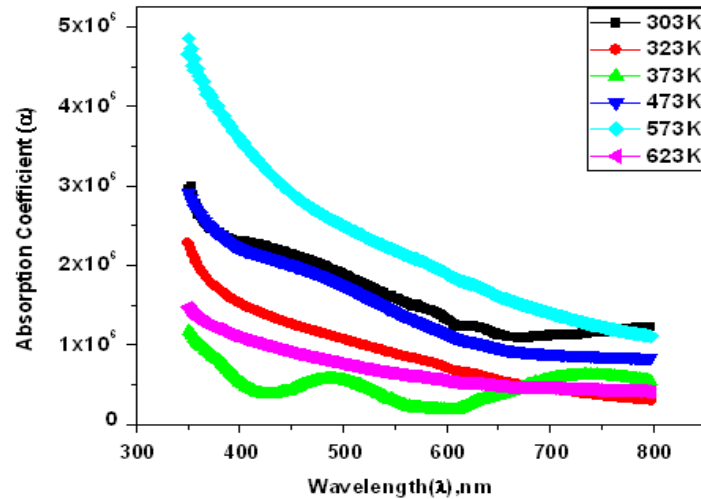


Fig 5. Plot of absorption coefficient ( $\alpha$ ) as a function of photon energy ( $h\nu$ ) for ZAO thin films at different substrate temperatures

The optical band gap,  $E_g$  is determined from the dependence of absorption coefficient values ( $\alpha$ ) on the photon energy, using Tauc's relation [30]

$$(\alpha h\nu) = B(h\nu - E_g)^n \quad (3)$$

where B is a parameter that depends on the transition probability,  $E_g$  is the optical band gap energy of the material,  $h\nu$  is the photon energy and n is an index that characterizes the optical absorption process and is theoretically equal to 2 and  $\frac{1}{2}$  for indirect and direct allowed transitions respectively. The optical band gap of the films was evaluated from the Tauc's plot of  $(\alpha h\nu)^2$  versus  $h\nu$  shown in figure 6.

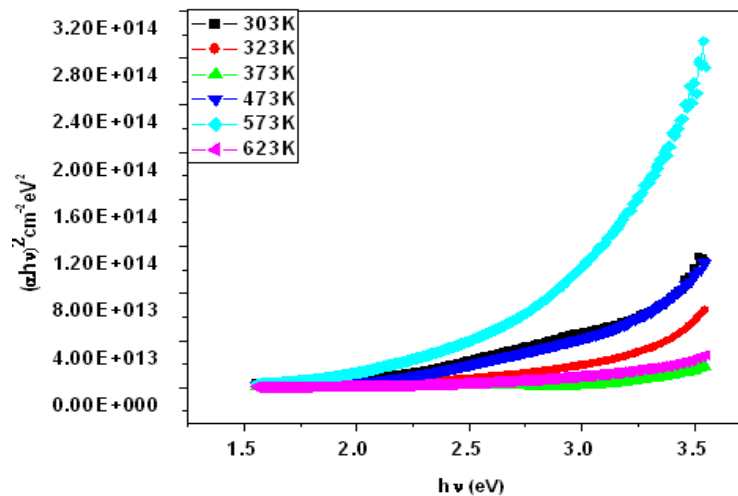


Fig 6. Variation of  $(\alpha h\nu)^2$  with  $h\nu$  as a function of substrate temperature

The estimated values of band gap from Tauc's plots are given in table 1. The increase of band gap with increase of substrate temperature is mainly related to the increase of carrier density. The maximum band gap is obtained for 623K. The change in optical band gap can be explain in terms of Burstein-Moss band gap widening and band gap narrowing due to the electron-electron and electron-impurity scattering [31-33].

Table 1: Optical band gap values of ZAO thin films deposited at various substrate temperatures

S.No	Substrate temperature,(K)	Optical band gap $E_g$ (eV)
1	303	3.30
2	323	3.37
3	373	3.43
4	473	3.25
5	573	3.17
6	623	3.42

The absorption coefficient near the fundamental absorption edge is exponentially dependent on the incident photon energy and obeys the empirical Urbach relation [34], where  $\ln \alpha$  varies as a function of  $h\nu$ .

$$\alpha = \alpha_0 \exp\left(\frac{h\nu}{E_u}\right) \quad (4)$$

where  $\alpha_0$  is a constant and  $E_u$  is Urbach energy, which is the width of the tails of localized state associated with the amorphous state in forbidden band. Thus, a plot of  $\ln(\alpha)$  vs.  $h\nu$  should be linear whose slope gives Urbach energy and is given in table 2. The Urbach's plots of the films are shown in figure 7.

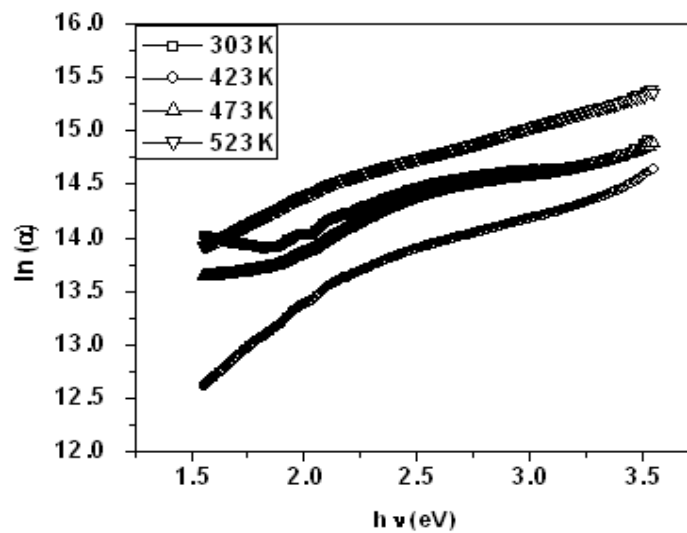


Fig 7. Urbach's plot for ZAO thin films deposited at different substrate temperatures

The dependence of the optical absorption coefficient with photon energy may arise from electronic transitions between localized states. The density of these states falls off exponentially with energy which is consistent the theory of Tauc [30, 35]. Equation (4) can be rewritten as,

$$\alpha(E) = \alpha_0 \exp \left[ \frac{\beta}{kT} (E - E_g) \right] \quad (5)$$

where  $\beta$  is a called steepness parameter, which characterizes the broadening of the absorption edge due to the electron-phonon interaction or excitation-phonon interaction. If the width of the edge is related to the slope of equation (4), the  $\beta$  parameter is found as  $\beta = kT/E_U$ , where  $k$  is Boltzmann constant and  $T$  is temperature in Kelvin. The  $\beta$  values calculated using this relationship and are given in table 2.  $E_U$  energy values change inversely with the optical band gap. Some defects during formation of film are formed. These defects produce localized states in the films.

Table 2: Urbach's energy ( $E_U$ ) and Steepness parameter ( $\beta$ ) values of ZAO thin films

S.No	Substrate Temperature, (K)	Urbach's energy $E_U$ (eV)	Steepness parameter( $\beta$ )
1	303	2.20	0.012
2	423	2.02	0.018
3	473	1.77	0.023
4	523	1.43	0.031

#### 4. Conclusions

Thin films of Zinc Aluminum Oxide were prepared by DC magnetron sputtering technique on glass substrates from 303K to 623K. From XRD patterns, ZAO thin films deposited on glass with substrate temperature from 303K-623K were preferentially oriented along the (0 0 2) direction. SEM images of ZAO have clear spherical grains of an average diameter of  $\sim 0.4$ - $1\mu\text{m}$ . The optical absorption spectra of the films show that the absorption spectra mechanism is due to direct transitions. The change in optical band gap ( $E_g$ ) is due to electron-electron and electron-impurity scattering. Optical band gap of ZAO thin films varies from 3.17-3.43eV. The Urbach energies ( $E_U$ ) and steepness parameters ( $\beta$ ) of the thin films are also reported.

#### Acknowledgements

The authors are thankful to UGC, New Delhi, India for financial support under the major research project (F.NO.37-346/2009, SR).

#### References

- [1] D.C.Look, Mater.Sci.Eng. B **80**, 382(2001).
- [2] H.Kind, H.Q.Yan, B.Messer, M.Law, P.D.Yang, Adv.Mater. **14**, 158(2002).
- [3] S.Suzuki, T.Miyata, M.Ishii, T.Minami, Thin Solid Films **434**, 14 (2003).
- [4] K. Ramanathan, M.A. Contreras, C.L. Perkins, S. Asher, F.S. Hasoon, J. Keane, D. Young, M.Romero,W. Metzger, R. Noufi, J.S. Ward, and A. Duda, Photovoltaics Res.Appl. **11**, 225 (2003).
- [5] J.S. Ward, K. Ramanathan, F.S. Hasoon, T.J. Coutts, J. Keane, M.A. Contreras, T. Moriarty R. Noufi, Photovoltaics Res.Appl. **10**, 41(2002).
- [6] J. Hüpkens, B. Recha, O. Kluth, T. Repmann, B. Zwaygardt, J. Muller, R. Drese, M. Wuttig, Solar Energy Mater. Solar Cells **90**, 3054 (2006).
- [7] A.Gupta, A.D.Compaan, Appl, Phys.Lett. **85**, 684 (2004).
- [8] G.Krirkids, M.Suchea, S.Christoulakis, N.Katsarakis, Rev.Adv.Mat.Sci. **10**, 215 (2005).



- [9] M.Sucnea, K.Christoulakis, N.Moschovis, G.Kasarakis, *Thin Solid Films* **515**, 551 (2006).
- [10] A.M.Gas'kov, M.N.Rumyantseva, *Russ. J.Appl.Chem.* **74**, 440 (2001).
- [11] N.G.Dhere, *Solar Energy Mater.Solar Cells* **90**, 2181 (2006).
- [12] N. F. Cooray, K. Kushiya, A. Fujimakaki, I. Sugiyama, T. Miura, D. Okumura, M. Sato, M. Ooshita and O. Yamase, *Solar Energy Mater. Solar Cells* **49**, 291 (1997).
- [13] Y.Hagiwara, T.Nakada, A.Kunioka, *Solar Energy Mater. Solar Cells* **67**, 267(2001).
- [14] O.Kluth, B.Rech, L.Houben, S.Wieder, G.Schoepe, C.Beneking, H.Wagner, A.Loeffl, H.W. Schock, *Thin Solid Films* **351**, 247 (1999).
- [15] B.Rech, O.Kluth, T.Repmann, T.Roschek, J.Springer, J.Mueller, F.Finger, H.Stiebig, H.Wagner, *Solar Energy Mater. Solar Cells* **74**, 439 (2002).
- [16] J.Mueller, B.Rech, J.Springer, M.Vanecek, *Solar Energy* **77**, 917 (2004).
- [17] J.Springer, B.Rech, W.Reetz, J.Mueller, M.Vanecek, *Solar Energy Mater. Solar Cells* **85**, 1 (2005).
- [18] J.H.Kim, K.C.Lee, C.Lee, *Proc. SPIE Int. Soc.Opt. Eng.* **49**, 5063 (2003).
- [19] T.M.Barnes, S.Hand, J.Leaf, C.A.Wolden, *J.Vac.Sci. Technol. A*, **22**, 2118(2004).
- [20] M.J.Alam and D.C.Cameron, *J.Vac.Sci. Technol.A*, **19**, 1642(2001).
- [21] J.M.Bian, X.M.Li, X.D.Gao, W.D.Yu, L.D.Chen, *Appl.Phys.Lett.* **84**, 541(2004).
- [22] T.Miyata, Y.Minamino, S.Ida, T.Minami, *J.Vac.Sci.Technol. A*, **22**, 1711(2004.)
- [23] B.Huang, S.Wu, J.Li, S.Sun, Z.O.Tian, *Proc.SPIE Int. Soc.Opt.Eng.* **38**,188(2005).
- [24] J.F.Chang, L.Wang, M.H.Hon, *J. Cryst. Growth* **211**, 93(2000).
- [25] J.H. Hou and M. Han, *J. Appl. Phys.* **71**, 4333 (1992).
- [26] J.Nishino, S.Ohshio and K.Kamata, *J.Am.Ceram.Soc.* **75**, 3469(1992).
- [27] J.F.Chang, C.C.Shen, M.H.Hon, *Ceram. Int.* **29**, 245(2003).
- [28] E.Marquez, J.Ramirez, P.Villares, R.Jimenez, P.J.S.Ewen, A.E.Owen, *J.Phys.D: Appl.Phys.* **25**, 535(1992).
- [29] Priyamvada Bharadwaj, P.K.Shishodia, R.M.Mehra, *J.Optoelectron.Adv.Mater.* **3**, 319 (2001).
- [30] J. Tauc, R. Grigorovici, A. Vancu, *Phys. Status Solidi* **15**, 627(1966).
- [31] E.Burstain, *Phys.Rev.* **93**, 638 (1954)
- [32] T.S.Moss, *Proc. Phys.Soc.Lond.: Ser. B* **67**, 775 (1954).
- [33] C.H.Peng, S.B.Desu, *J.Am.Ceramic.Soc.* **77**, 929(1994).
- [34] F. Urbach, *Phys. Rev.* **92**, 1324 (1953).
- [35] G.D. Cody, T. Tiedje, B. Abeles, Y. Goldstein, *Phys. Rev. Lett.* **47**, 1480 (1981).